ELSEVIER

International Journal of Heat and Fluid Flow 22 (2001) 272–278

International Journal of HEAT AND FLUID FLOW

www.elsevier.com/locate/ijhff

# Unsteady heat transfer in subsonic boundary layers

R. Schook *, H.C. de Lange, A.A. van Steenhoven

*Department of Mechanical Engineering, Eindhoven University of Technology, P.O. Box 513, 5600 MB Eindhoven, Netherlands*

**Abstract**

Unsteady boundary layer transition experiments are performed in a modified Ludwieg tube setup. The transition is initiated by means of a moving bar mechanism which translates cylinders in front of a test plate. The intensity of the wakes shed by the cylinders is so large that transition starts at the leading edge. In streamwise direction the wake-induced transition area grows and keeps its initial shape. Also experiments are performed in which the moving cylinders are combined with a static grid. In the time between two wakes, individual turbulent spots develop which grow in streamwise direction. These spots merge with the wake-induced transition until a completely turbulent boundary layer is obtained. When the experimental results are transformed in intermittency distributions based on the turbulent-to-laminar time fraction, the superposition principle proofs to be applicable. However, the intermittency distribution based on the mean heat flux cannot be determined unequivocally. This is due to the fact that there does not exist a unique turbulent heat flux. This flux appears to be dependent on the origin of the transition. 

## 1. Introduction

Laminar-to-turbulent transition in a boundary layer has a large effect on the heat transfer. The flux in a turbulent layer is much larger than in a laminar layer under the same conditions. Several parameters influence transition (Narasimha, 1985; Mayle, 1991), most important are the turbulence level, turbulence length scale and pressure gradient effects. When the turbulence level increases the transition starts earlier. Also the transition length, i.e., the distance it takes in streamwise direction to obtain a fully turbulent flow, decreases.

Another feature which influences transition is unsteady flow; moving wakes initiate transition as they flow along a surface. The turbulence in the wake is much larger than the free stream turbulence, so when a wake passes, the transition start shifts towards the leading edge. As a result the total (time averaged) heat flux is higher than that of a flow without wakes (Funazaki et al., 1993). Boundary layer transition initiated by wakes often is called wake-induced transition. This type of transition is very important for turbomachinery design. Stator blades shed wakes which are convected along the rotor blades positioned downstream. So, the rotor blade is subjected to an unsteady flow which, part of the time, consists of the main flow, and part of the time consists of wakes.

This paper describes the results of transition measurements along a flat plate. The experiments are performed in a (modified) Ludwieg tube setup. In this facility a well-defined and high velocity flow is generated for a short time (Hogendoorn, 1997). First the experimental setup is described. Then, the hot-wire measurements are treated. With these results the main stream turbulence in the flow is characterized. Also the velocity deficit behind the wake is determined.

After that, the heat flux experiments are presented for steady, unsteady and combined transition experiments. Special attention is given to the 'turbulent' flux level.

Finally, the boundary layer transition for several cases are compared by transforming the results in intermittency distributions.

## 2. Experimental setup: the Ludwieg tube

A transient flow is generated by a Ludwieg tube (Fig. 1). This setup consists of a tube connected via the test section to a dump tank. The test section and the dump tank are separated by a diaphragm and a choking orifice. Prior to an experiment the pressure in the dump tank is brought to about 300 Pa while the pressure in the tube and test section is set to the initial value, depending on the Reynolds number required. The experiment commences when the diaphragm is ruptured. A shock wave travels in the dump tank and an expansion wave travels to the end of the tube and back. During this time expanded gas flows through the test section and the measurements are performed.

A major advantage of this setup is that the Mach number and the Reynolds number can be adjusted independently. The Mach number is determined by the geometry, i.e., the area of the choking orifice. The Reynolds number is set by altering the initial pressure in the tube. To measure the local heat fluxes to the test plate, a sensor plate is mounted in the section. Pressure measurements can be performed above the leading edge of the plate and in the tube itself, just in front of the test section. The

* Corresponding author. Tel.: +31-40-247-2320; fax: +31-40-243-3445.

*E-mail address:* r-schook@hotmail.com (R. Schook).

0142-727X/01/$ - see front matter 
PII: S0142-727X(01)00102-3

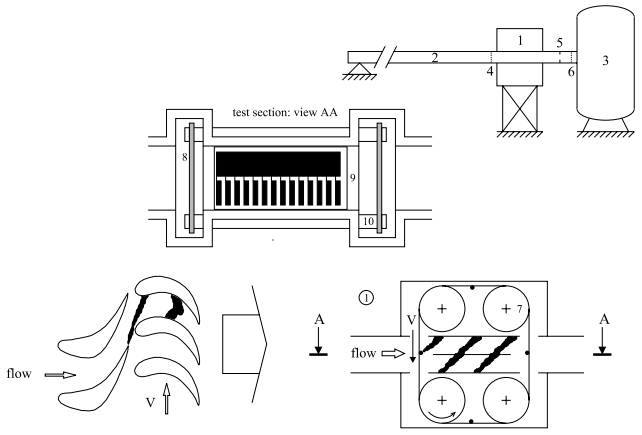


Fig. 1. Experimental setup: the Ludwieg tube. 1: Test section, 2: tube, 3: dump tank, 4: turbulence grid, 5: choking orifice, 6: diaphragm, 7: disc, 8: cylinder, 9: sensor plate, 10: belt.

hot-wire probe for measuring the turbulence characteristics is situated 27 mm in front of and 10 mm above the sensor plate; this position is chosen such that the wire does not disturb the boundary layer developing on the plate.

Turbulence can be generated in two different ways. The first possibility is by using static grids which consists of bars with a diameter $D$ and a mesh size $m$. The values for the grid used for the experiments described in this paper are: $D = 1$ mm and $m = 12.5$ mm It is positioned 167 mm in front of the leading edge of the test plate. This grid, denoted by the 1H-grid, generates turbulence resulting in 'steady' bypass transition.

The second way of generating turbulent disturbances in the flow is by using a special wake generator (see Fig. 1). This generator consist of two belts, conveying cylinders 40 mm in front of the test plate. The speed of the translating cylinders, denoted by $V$, has a maximum of 35 m/s, while the free stream velocity is 110 m/s for all the experiments. ($Ma = 0.33$). This results in a maximum flow coefficient (the ratio of cylinder speed and the free stream velocity) of 0.3.

Now a distinction is made between unsteady and combined transition. Moving cylinders in a flow with a low background turbulence level (no turbulence grid included) cause 'unsteady' transition. The case of both a turbulence generating grid and moving cylinders will be referred to as 'combined' transition.

## 3. Important parameters for unsteady transition

The important parameters for the unsteady transition process are shown schematically in Fig. 2. The ratio of the

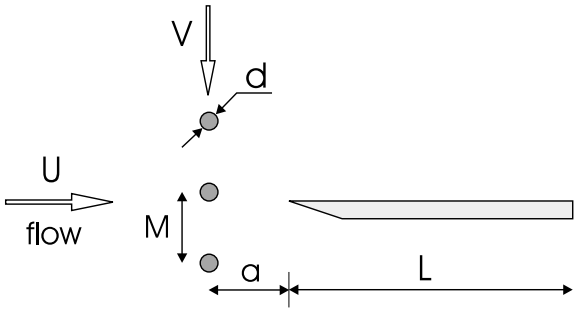


Fig. 2. Important parameters for unsteady transition.

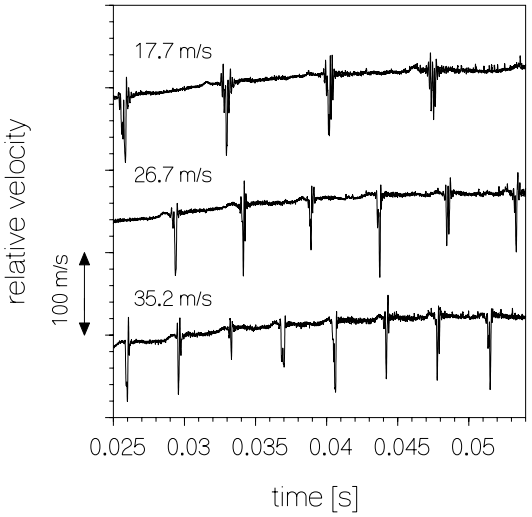


Fig. 3. Relative velocity for twelve cylinders with a diameter of 3 mm. Velocities $V$ are 17.7, 26.7 and 35.2 m/s; no turbulence generating grid is included.

main stream velocity $U$ and the cylinder translating velocity $V$ determines the unsteadiness of the flow, i.e., the flow coefficient: $\Phi = V/U$.

The diameter of the cylinders is $d$ and the distance between different cylinders is the mesh size $M$. Parameter $a$ is the distance between the center of the cylinders and the leading edge of the test plate (length $L$) which is adjusted to 40 mm for all the experiments described. The strength of the wakes is determined by $d$ (for the present measurements the diameter is 5 or 3 mm). Large diameters result in strong wakes and an early transition start. The ratio of length scales which determine this process is: $d/a$.

For weaker wakes [1] the transition start shifts downstream. In this case a more important ratio is probably $d/\delta$, with $\delta$ the local boundary layer thickness determined by the local position $x$. So, independent characterizing parameters are $d/x$ and $Re_x$.

The mesh in combination with the velocity $V$ characterizes the wake passing frequency $f$. From $f$, the Strouhal number, which is a measure for the unsteadiness, is introduced

$$S = \frac{\ell f}{U}. \tag{1}$$

In this equation $\ell$ is an involved length, e.g., the length of the test plate.

## 4. Hot-wire signals

Hot-wire measurements are performed to determine the turbulence level and the velocity deficit behind the moving cylinders. Velocity signals for an unsteady transition experiment, in which only moving cylinders are present, are given in Fig. 3. This figure shows the velocities for twelve cylinders with a diameter of 3 mm. (Note that the three signals (different cylinder velocity) are shifted vertically.) It is seen that in the case of $V = 17.7$ m/s, four cylinder (thus wake) passings are present during the test time, while eight wake passings are present when $V = 35.2$ m/s. For getting an idea of the velocity

[1] Weak wakes, i.e., wakes which give a start of transition after the leading edge, are not subject of this paper.

deficit behind the cylinder: five divisions correspond with a velocity difference of about 100 m/s, (as indicated in the figure). From the fluctuations between two wakes the background turbulence is calculated. In this case (without a static turbulence grid), the turbulence level is about 0.25%.

## 5. Heat flux measurements

The heat fluxes are measured using a thin film technique. Titanium sensors with a thickness of 70 nm are evaporated at the top of a sensor plate made of glass with well-known properties. In total 14 sensors with a streamwise distance of 10 mm are used in the present experiments. The first sensor is positioned 2 mm behind the leading edge.

The sensor resistance depends on the sensor temperature by

$$R_g = R_0[1 + \alpha_0(T_g - T_0)]. \quad (2)$$

Values of $R_0$ and $\alpha_0$ are determined by calibration. All sensors are part of a separate Wheatstone bridge. When the sensor temperature changes, the sensor resistance changes and the bridge becomes unbalanced. The resulting signal is amplified by an operational amplifier and recorded at a frequency of 50 kHz.

The temperature distributions in the test plate, perpendicular to its surface, are reconstructed for each sensor by solving the one-dimensional heat conduction equation. The boundary conditions used to solve this equation are the top temperature at the plate, i.e., the sensor temperature, and a constant temperature for the bottom of the plate. The latter condition is valid as long as the thermal front does not reach the bottom (1 s after starting the experiment). While the complete experiment only takes 0.1 s it is allowed to use this assumption. Finally, the heat flux is calculated by using Fourier's law.

## 6. Transition results

Unsteady transition experiments are performed for moving cylinders with a diameter of 5 and 3 mm. The relative heat fluxes for seven different sensors in streamwise direction are shown in Fig. 4. These fluxes are plotted on the same vertical ordinate but shifted vertically (one division in vertical direction equals 0.2 kW/m$^2$). Figs. 4(a) and (b), respectively, show the influence of four and eight passing cylinders ($d = 5$ mm). The corresponding cylinder velocities are 17.7 and 35.2 m/s. The same figures are given for 3 mm cylinders (Figs. 4(c) and (d)). It is seen that as a cylinder passes the leading edge of the test plate, the heat transfer increases. The disturbances initiated by the cylinders have such strength that transition starts at the leading edge of the plate, i.e., when the wake passes, the boundary layer becomes turbulent instantaneously (resulting in the flux increase). In streamwise direction, the shape of the heat transfer increase seems to remain the same. However, the size of the turbulent region enlarges, so the leading edge velocity of the wake is larger than the trailing edge velocity. For the 5 mm cylinders the wake width is larger than for the 3 mm cylinders. In the present configuration the number of cylinders is not large enough to obtain a fully turbulent boundary layer caused by (solely) unsteady transition.

Steady and combined experiments are also performed. These measurements are done with a static turbulence generating grid which generates homogeneous background turbulence. The resulting turbulence level 27 mm in front of the leading edge is 1.15%.

Fig. 5 shows the heat flux as a function of time for the case of non-moving cylinders but with a static turbulence grid positioned upstream of the plate (1H-grid). The output for the first three sensors indicates a laminar boundary layer. The fourth sensor ($Re_x = 2.16 \times 10^5$) shows some spikes at random

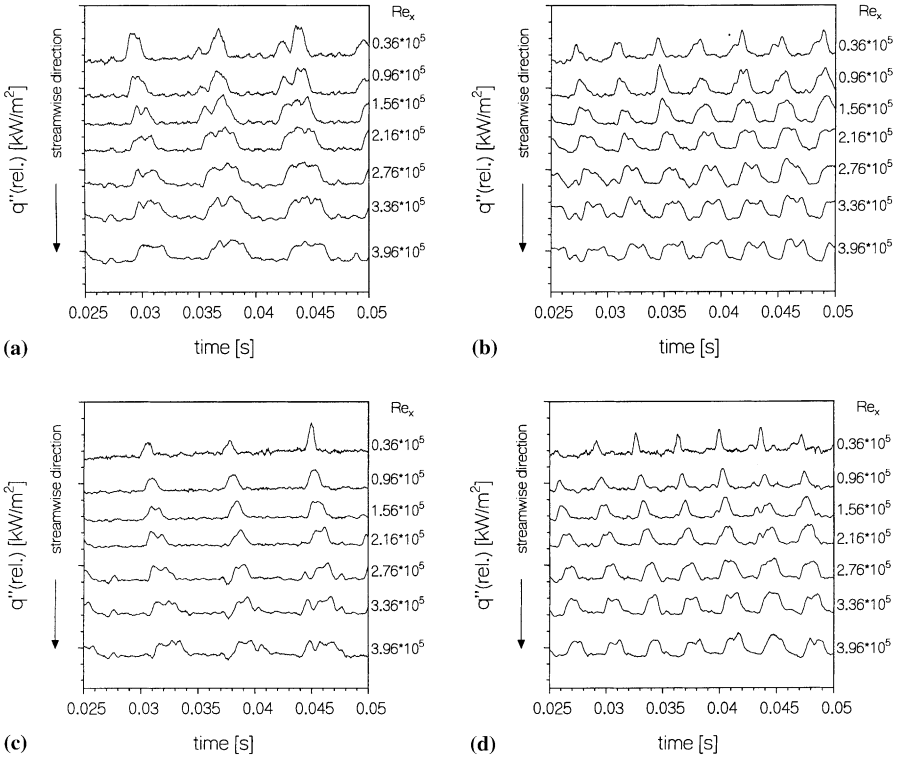


Fig. 4. Heat fluxes for several sensors in streamwise direction. No turbulence grid is included; $Re_u = 3.0 \times 10^6$ m$^{-1}$. (a) $V = 17.7$ m/s, $d = 5$ mm; (b) $V = 35.2$ m/s, $d = 5$ mm; (c) $V = 17.7$ m/s, $d = 3$ mm; (d) $V = 35.2$ m/s, $d = 3$ mm.

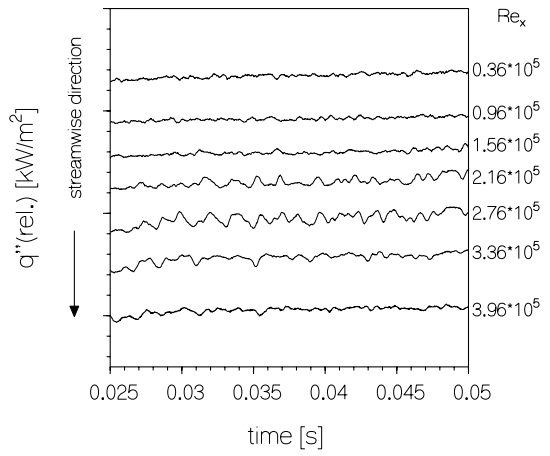


Fig. 5. Heat fluxes for several sensors in streamwise direction. Turbulence grid 1H included (steady transition).

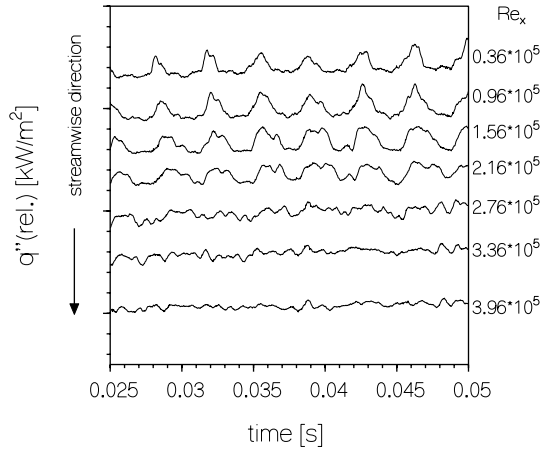


Fig. 6. Heat fluxes for several sensors in streamwise direction. Turbulence grid 1H included (combined transition).

positions in time. Further downstream, these spikes grow and merge until a complete turbulent boundary layer is obtained. The spikes are better known as turbulent spots (Emmons, 1951).

Fig. 6 shows the experiment with both a static grid and moving cylinders. Between two passing wakes turbulent spots start to develop. These spots merge and combine with the wake-induced turbulence until a fully turbulent boundary layer is obtained. When the free stream turbulence is small (e.g., in the case of no static grid) the boundary layer relaminarizes between two passing wakes. However, when the background turbulence is high enough the transition process is a combination of wake-induced transition and 'static' bypass transition (due to the static grid).

## 7. Mean heat flux

It can be derived analytically that the Stanton number for a laminar Blasius boundary layer equals (Schlichting, 1979)

$$St_l = 0.322 Pr^{-2/3} Re_x^{-1/2}. \quad (3)$$

For fully developed turbulent boundary layers an empirical Stanton number relation is known (Kays and Crawford, 1980)

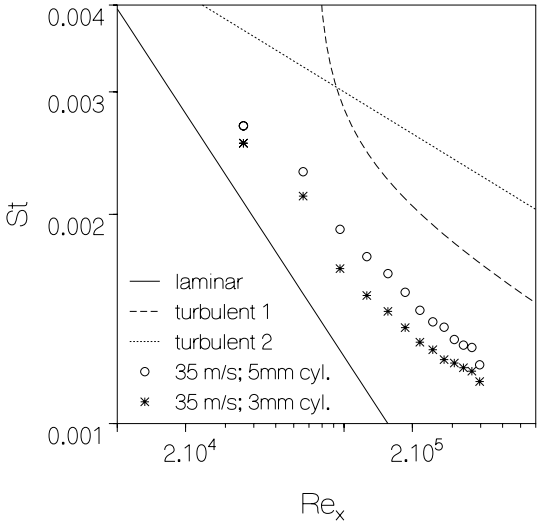


Fig. 7. Mean heat flux for unsteady experiments at a velocity of 35 m/s (twelve 5 mm cylinders and twelve 3 mm cylinders); 'turbulent 1' curve: Eq. (5); 'turbulent 2' curve: Eq. (4).

$$St_t = 0.0287 Pr_t^{-0.4} Re_x^{-0.2} = C Re_x^{-0.2}. \quad (4)$$

For a turbulent Prandtl number of 0.9 the constant $C$ becomes 0.030. Another relation for the Stanton number, which accounts for the fact that turbulence in the boundary layer has to develop, is

$$St_t = C Re_{x-x_t}^{-0.2}. \quad (5)$$

The constant $C$ is obtained by applying a data fit through the turbulent part of the heat flux distribution (of the 1H transition case) and $x_t$ is the transition start.

Fig. 7 shows the mean heat flux in terms of the Stanton number for the unsteady experiment of 5 and 3 mm cylinders. Also the turbulent curves are depicted (Eqs. (4) and (5)). It is seen that the mean heat flux for the 5 mm cylinders is larger than that of the 3 mm cylinders, which is caused by the larger wake width.

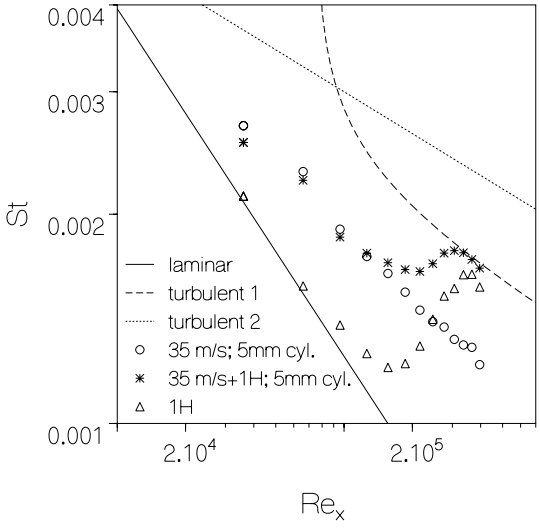


Fig. 8. Mean heat flux for an unsteady experiment, a steady experiment and a combined experiment (1H turbulence grid); 'turbulent 1' curve: Eq. (5); 'turbulent 2' curve: Eq. (4).

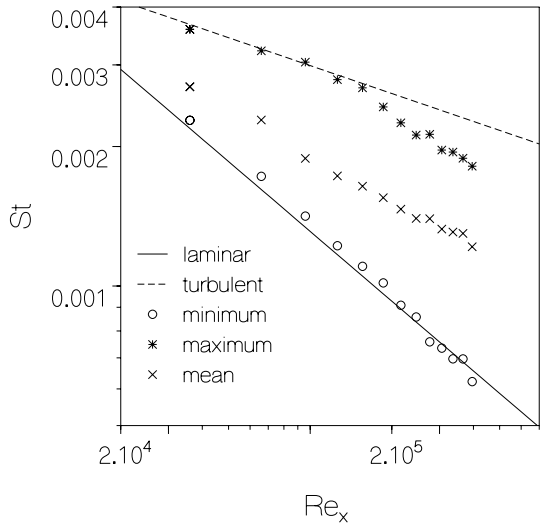


Fig. 9. Minimum, maximum and mean heat fluxes for the unsteady experiments with 5 mm cylinders at a velocity of 35 m/s; $Re_u = 3.0 \times 10^6$ m$^{-1}$; laminar curve: Blasius; turbulent curve: $St = 0.03Re_x^{-0.2}$, i.e., $Pr_t = 0.9$.

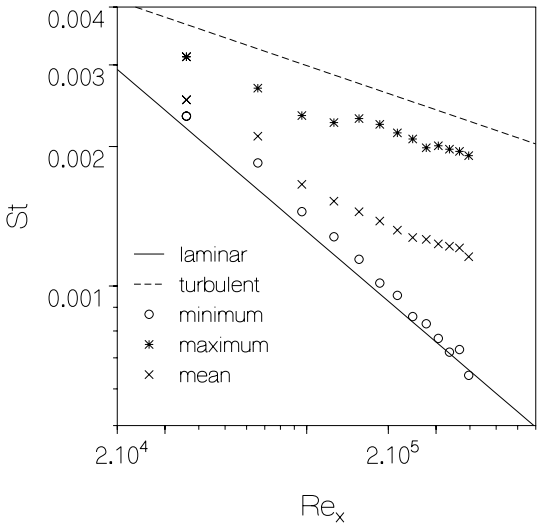


Fig. 10. Minimum, maximum and mean heat fluxes for the unsteady experiments with 3 mm cylinders at a velocity of 35 m/s; $Re_u = 3.0 \times 10^6$ m$^{-1}$; laminar curve: Blasius; turbulent curve: $St = 0.03Re_x^{-0.2}$, i.e., $Pr_t = 0.9$.

In Fig. 8 the flux for the steady, unsteady and combined experiment are given. The steady transition is seen to have the classical 'S'-shape, which agrees with the Narasimha transition model (Narasimha, 1985; Schook et al., 2001). For this situation the 'turbulent' flux, given by Eq. (5), is reached when transition is completed. Also it is observed that the combined experiment has a larger mean flux than a steady or unsteady experiment alone. In Mayle and Dullenkopf (1990) it is argued that both spot production processes behave independently, and thus spots initiated by unsteady and steady transition can be superposed. This results in an increase of the number of spots, and, therefore, in an increase of the heat flux.

## 8. Maximum turbulent heat flux

The influence of the wake strength on the heat transfer is determined from the flux signal as a function of time. The minimum and the maximum heat flux during the test time are calculated.

The results for the unsteady experiments are depicted in Figs. 9 and 10 (the according time dependent flux signals are depicted in Figs. 4(b) and (d)). Also the laminar (Eq. (3)) and the turbulent (Eq. (4)) curves are shown. It follows that for the 5 mm cylinders and the 3 mm cylinders, the minimum heat flux agrees well with the value for a laminar boundary layer. This means that in between two wake passages the flow relaminarizes. The maximum heat flux (which occurs during a wake passage) is seen to differ for both cases. For the 5 mm cylinders the 'turbulent' heat flux follows Eq. (4) with $C = 0.03$ accurately until a Reynolds number of $1.5 \times 10^5$ is reached. After this streamwise position, the turbulent flux starts to become smaller than the flux according to Eq. (4).

## 9. Intermittency distributions

The original definition of the intermittency is the fraction of time in which the flow is turbulent at a certain streamwise position. If turbulent events can be recognized in for example a hot-wire or heat flux signal, the intermittency can be determined by taking the time period of these turbulent events. In this section, the intermittency calculated by this method will be referred to as the time-based intermittency: $(\gamma_t(x))$. For the unsteady transition measurements $\gamma_t$ can be determined. For this, a threshold heat flux of $St_* = 0.5(St_{max} + St_{lam})$ is used. If the heat flux has a higher value than $St_*$, the flow is assumed to be turbulent.

When the laminar and turbulent heat flux are known, the flux-based intermittency: $(\gamma_f(x))$ can be determined from

$$\gamma_f(x) = \frac{\overline{St(x)} - St_l(x)}{St_t(x) - St_l(x)}. \tag{6}$$

To determine $\gamma_f$, Eq. (3) is applied for the laminar heat flux, while the maximum heat flux, i.e., $St_t(x) = St_{max}(x)$, is used for the turbulent heat flux.

Both $\gamma_t$ and $\gamma_f$ for twelve 5 and 3 mm cylinders moving at a velocity of 35.2 m/s, are shown in Fig. 11. It is seen that wake-induced transition starts at the leading edge. Therefore, the intermittency has a non-zero value close to the leading edge (i.e., at low $Re_x$). This holds for the 5 mm cylinders and the 3 mm cylinders. Disregarding the first part of the intermittency (until $Re_x = 1 \times 10^5$), the intermittency increases in streamwise direction. The intermittency is always higher for the 5 mm cylinders than it is for the 3 mm cylinders.

The transition process occurs by the initiation and growth of turbulent spots. If a turbulent spot is supposed to behave as a local area of fully turbulent flow, the local heat flux in the spot should have the 'turbulent' value. If a unique 'turbulent' heat flux can be defined, the $\gamma_t$ and $\gamma_f$ should be the same. Fig. 11 shows that there is indeed a reasonable agreement for both intermittencies. (Note that the conclusion can be influenced by using another threshold value in the definition of $\gamma_t$.)

Suppose that spots can originate from two different sources. The first one is initiation due to natural (or bypass) transition, while the second is the initiation by wake-induced transition. When both contributions are independent, it is shown by Mayle and Dullenkopf (1990) that the intermittency can be written as

$$\tilde{\gamma}(x) = \gamma_n(x) + \tilde{\gamma}_w(x) - \gamma_n(x)\tilde{\gamma}_w(x). \tag{7}$$

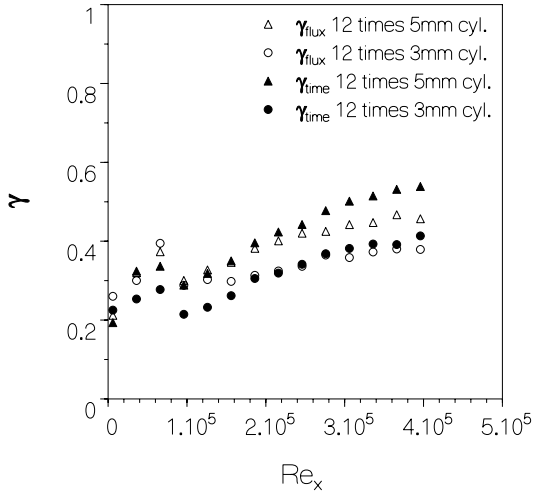


Fig. 11. Flux-based intermittencies (open symbols) and time-based (closed symbols) intermittencies for twelve 5 and 3 mm cylinders; $V = 35.2$ m/s.

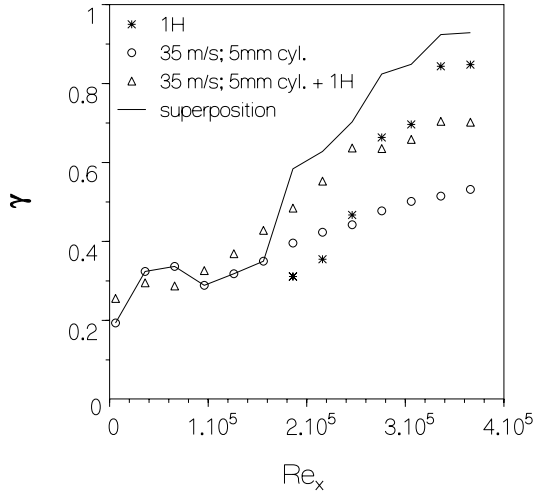


Fig. 13. Flux-based intermittencies for steady, unsteady and combined transition; also the superposition of turbulent spots is shown.

In this equation $\gamma_n(x)$ is the intermittency for natural (or bypass) transition, while the contribution of the wakes is incorporated in the term $\tilde{\gamma}_w(x)$.

For steady, unsteady and combined transition experiments, $\gamma_t$ and $\gamma_f$ are compared in Figs. 12 and 13. Also the intermittency which follows from the superposition principle applied to the steady and unsteady measurements (Eq. (7)) are shown. The curves depicted in Fig. 12 are roughly as expected. The combined experiment gives an intermittency which is higher than the steady and unsteady experiments. Furthermore, the trend of the intermittency according to the superposition, follows the measurements (compare the full line to the triangles).

However, the superposition principle fails if it is applied to $\gamma_f$. It is seen (Fig. 13) that for higher $Re_x$ values the intermittency of the steady experiment is larger than the intermittency of the combined experiment. For combined transition the number of spots, and thus the intermittency, must be larger. It is obvious that this contradicts with reality. The reason for this discrepancy is the difference in the applied turbulent heat flux levels. As the maximum turbulent heat flux of the steady experiment is less than the maximum heat flux of unsteady experiment, the superposition can not be applied unequivocally. Therefore, any flux-based intermittency in a combined experiment must be used with extreme care. The only possibility to obtain an unambiguous flux-based intermittency, is to report the flux level(s) on which the intermittency is based. However, with this restriction the advantage of the intermittency, i.e., describing the state of the boundary layer in a unique manner, disappears.

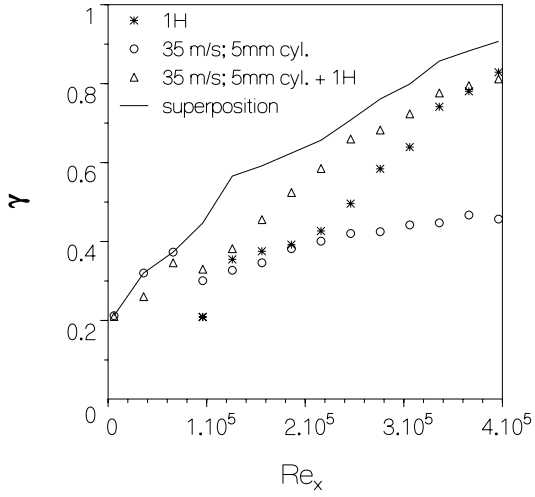


Fig. 12. Time-based intermittencies for steady, unsteady and combined transition; also the superposition of turbulent spots is shown.

## 10. Conclusions

It is shown that strong wakes can be generated in the Ludwieg tube setup. These wakes initiate transition which starts at the leading edge of the test plate. The initial shape of the wake remains recognizable in the heat flux signals. Increasing the flow coefficient ($V/U$), i.e., increasing the cylinder velocity, results in a decrease of the width of the wake. When the cylinder diameter is increased the wakes become stronger, resulting in larger wake widths.

Combined transition experiments show that the turbulent spots originating from steady and unsteady transition merge with each other until a complete turbulent boundary layer is obtained. As a result, the mean heat flux of a combined experiment is larger than the flux of a steady or unsteady experiment alone.

For the unsteady transition resulting from strong wakes, it is found that the time-based intermittency and the flux-based intermittency roughly coincide.

The minimum heat flux for unsteady experiments equals the value belonging to a laminar boundary layer. Therefore, it is derived that in between two wake passages the flow relaminarizes. The maximum (turbulent) heat flux depends on the cylinder diameter. When this diameter is enlarged the maximum heat flux increases. From this it follows that a unique 'turbulent' heat flux (in terms of $St$) does not exist. So, it is not possible to define a flux-based intermittency, and thus the state of the boundary layer, without taking into account the effect of wake passages on the turbulent heat flux.

## References

Emmons, H.W., 1951. The laminar–turbulent transition in a boundary layer. J. Aero. Sci. 18, 490–498.

Funazaki, K., Meguro, T., Yamawaki, S., 1993. Studies on the unsteady boundary layer on a flat plate subjected to incident wakes. JSME Int. J. B 36, 532–539.

Hogendoorn, C.J., 1997. Heat transfer measurements in subsonic transitional boundary layers. Ph.D. thesis, Eindhoven University of Technology.

Kays, W.M., Crawford, M.E. (Ed.), 1980. Convective Heat and Mass Transfer. McGraw-Hill, New York, pp. 1980.

Mayle, R.E., 1991. The role of laminar-turbulent transition in gas turbine engines. J. Turbomach. 113, 509–537.

Mayle, R.E., Dullenkopf, K., 1990. A theory for wake-induced transition. J. Turbomach. 112, 188–195.

Narasimha, R., 1985. The laminar–turbulent transition zone in the boundary layer. Prog. Aero. Sci. 22, 29–80.

Schlichting, H. (Ed.), 1979. Boundary Layer Theory. McGraw-Hill, New York, pp. 1979.

Schook, R., Lange, H.C., van Steenhoven, A.A., 2001. Heat transfer measurements in transitional boundary layers. Int. J. Heat Mass Transfer 44, 1019–1030.